Shear band formation in granular materials: a micromechanical approach

Ana María Gómez Gómez* / Arcesio Lizcano Peláez**

Fecha de envío: 25 de enero de 2009.
Fecha de aceptación: 27 de febrero de 2009.

Abstract

Shear bands as mode of failure in granular soils has been largely studied without to physically explain the formation mechanism of that, neither to reproduce exactly a defined failure pattern. Several algorithms were performed with a distinct element method. In this ones, are looking for to reproduce only shear band in a biaxial simulation on rigid disk assembly, to get information at shear zone.

Keywords: Shear bands, micromechanics, granular materials, biaxial test, PFC2D, simulation, particulate materials

Formación de bandas de corte en materiales granulares: una aproximación micromecánica

Resumen

Las bandas de corte como modo de falla de suelos granulares han sido ampliamente estudiadas sin explicar físicamente su mecanismo de formación ni reproducir con exactitud un patrón de falla definido. Se desarrollaron varios algoritmos usando un método de elementos discretos, en los que se buscó reproducir la formación de una banda de corte única en una simulación de un ensayo biaxial sobre un ensamblaje de discos rígidos, para obtener información de esfuerzos en la zona de corte.

Palabras clave: Bandas de corte, micromecánica, materiales granulares, prueba biaxial, PFC2D, simulación, materiales particulados

* Ingeniera de Diseño Ingetec Ingeniería y Diseño S. A. Correo electrónico: anagomez@ingetec.com.co

** Director del Departamento de Ingeniería Civil y Ambiental de la Universidad de los Andes. Correo electrónico: alizcano@uniandes.edu.co

Introduction

In a plane strain compression on dense sands, homogeneous deformation first takes place. Near peak stress, the deformation suddenly localizes into thin zones (called shear bands), and the stress drops to a residual stress state. In soil mechanics, this mode of failure is very important as well as in engineering design problems, where one is interested in ultimate and residual bearing capacities of the analyzed structures.

To study shear bands, Hill (1962) Mandel (1964) and Rudnicki & Rice (1975) analyzed the occurrence and inclination of shear bands. But, their constitutive equations are function only on the first gradient of displacement then the shear band thickness is undetermined. Mühlhaus & Vardoulakis used the Cosserat theory to obtain the shear band thickness as a material length, but Huang & Bauer (2001) and Tejchman & Gudehus (2001) showed that the thickness of shear bands is not a material constant. Huang et al. (2002) find that the thickness of shear bands is proportional to the mean grain diameter and a friction parameter related with inter-granular friction and these one is influenced by the density and stress rate. In all cases, the analyses are developed in plane strain conditions with constitutive equations in 2D and supported with quantities of stress and strain at the boundary of the biaxial specimens but they did not consider the micro-structure behavior and this relation with the localization of deformation process. Several authors has develop studies related with the microstructure of shear bands: Bardet & Proubet (1992) with numerical simulations of granular assemblies suggest that the particle rotations at shear bands are induced by macrorotations, Iwashita & Oda (1998) and Oda & Kazama (1998) showed with numerical simulation that the microdeformation mechanism of dilatancy in a shear band is the combination of buckling and rolling of columns, but do not mention about the implementation algorithm to boundary conditions. To develop parametric studies of the influence of initial density, load velocity and stiffness at contacts it is necessary first to have an algorithm that permit to reproduce realistic biaxial test with particle assemblies. In this paper, two algorithms to reproduce flexible boundaries (like membranes) are presented. The goal of the work is to develop a deeper understanding of the micromechanics of particle assemblies (Gómez, 2004).

Discrete model

The discrete model employed to implement the soft boundary algorithm was the commercially available code PFC-2D v3.0 (Itasca, 2002, b). The mathematical formulation is based upon the solution of Newton's equations of motion for each particle in a two-dimensional assembly.

The assumptions of method are: contacts occur at a point, particles may be represented as rigid disks or spheres, and particle overlap is allowed at contacts but these overlaps are small relative to particle size. The solution include: law of motion, force-displacement law, as part of calculation cycle, and contact constitutive model and boundary conditions that defines the simulation conditions and last ones are user defined.

Force-displacement law

Solution of the problem begins with determining the unit normal vectors of the contacts in the assembly as:

$$n_i = \frac{x_i^{[B]} - x_i^{[A]}}{d} \qquad (1)$$

where: n_i is the normal vector; $x_i^{[A]}$ and $x_i^{[B]}$ are the locations of particle centers A and B, respectively, and d is the distance between particle centers. The overlap at contacts, U^n, is calculated as:

$$U^n = \begin{cases} R^{[A]} + R^{[B]} - d \\ R^{[B]} - d \end{cases} \quad (2)$$

In first case Eq. (2) defines the overlap between two ball and the second one the overlap between ball and wall; $R^{[\Phi]}$ is the radius of ball Φ and d is the distance between two centers of contiguous particles. The location of the contact point is:

$$x_i^{[C]} = \begin{cases} x_i^{[A]} + \left(R^{[A]} - \tfrac{1}{2}U^n\right)n_i \\ x_i^{[B]} + \left(R^{[B]} - \tfrac{1}{2}U^n\right)n_i \end{cases} \quad (3)$$

When contact location is known, it is possible to calculate velocities and invoke the constitutive relation for contact theory to calculate normal and shear forces on each particle.

Motion law

Each new calculation cycle, new particle forces, F_i, and moments, M_3, are used to calculate the new acceleration and angular momentum, and then the Newton's equations of movement are applied:

$$F_i = m(\dot{x}_i - g_i) \quad (4)$$

$$M_i = \dot{H}_i \quad (5)$$

where m is particle velocity, g_i is acceleration due to gravity, H_i is the angular momentum of the particle and β is 0.4 for spheres and 0.5 for disks. The equations of motion 4 and 5 are discretized with central finite differences:

$$\begin{aligned} \dot{x}_i &= \frac{1}{\Delta t}\left(\dot{x}_i^{(t+\Delta t/2)} - \dot{x}_i^{(t-\Delta t/2)}\right) \\ \dot{\omega}_3 &= \frac{1}{\Delta t}\left(\omega_3^{(t+\Delta t/2)} - \omega_3^{(t-\Delta t/2)}\right) \end{aligned} \quad (6)$$

$$\begin{aligned} \dot{x}_i^{(t+\Delta t/2)} &= \dot{x}_i^{(t-\Delta t/2)} + \left(\frac{F_i^{(t)}}{m} + g_i\right)\Delta t \\ \omega_3^{(t+\Delta t/2)} &= \omega_3^{(t-\Delta t/2)} + \left(\frac{M_3^{(t)}}{I}\right)\Delta t \end{aligned} \quad (7)$$

$$x_i^{(t+\Delta t)} = x_i^{(t)} + \dot{x}_i^{(t+\Delta t/2)}\Delta t \quad (8)$$

the equations 6 to 8 are respectively, translational and rotational accelerations, translational and rotational velocities, and displacement.

The critical value of the time step for a stable solution to a DEM problem depends on the minimum eigenperiod of the entire system. Calculating this value is computationally very expensive, so PFC-2D uses a simplified spring and mass logic to calculate the critical time step (Itasca, 2002):

$$t_{crit} = \begin{cases} \sqrt{m/k^{tr}} \\ \sqrt{I/k^{r}} \end{cases} \quad (9)$$

where m and I are the mass and inertia of particle, and k^{tras} and k^{rot} are the translational and rotational stiffnesses. The minimum of all critical timesteps computed for all degrees-of-freedom of all particles is the final critical timestep.

Contact model

The contact model relates relative displacements with contact forces via Eqs. 10 and 11:

$$F_i^n = K^n U^n n_i \quad (10)$$

$$\Delta F_i^s = -k^s \Delta U_i^s \quad (11)$$

The normal stiffness, K^n, is secant stiffness and it relates the total normal force to the total normal displacement; the shear stiffness, k^s, is a tangent stiffness since it relates the increment of shear displacement to the increment of shear force. The contact normal and shear stiffnesses are given by:

$$K^n = \frac{k_n^{[A]} k_n^{[B]}}{k_n^{[A]} + k_n^{[B]}} \tag{12}$$

$$k^s = \frac{k_s^{[A]} k_s^{[B]}}{k_s^{[A]} + k_s^{[B]}} \tag{13}$$

In PFC-2D program, this model as referred as linear contact model.

Boundary conditions

In PFC-2D it is possible to define boundary conditions by two kinds of control entities: velocity-controlled walls or velocity or force-controlled particles.

Program environment

PFC-2D has a series of commands that permit to create and deal with the model entities as particles and walls, and a programming language called fish, with their own language rules and intrinsic functions, and that enables the user to define new functions and to generate his own control boundary conditions to program simulation environments. Itasca as support codes of fish has some test environments and models called "Augmented fishtank", to develop a biaxial test, but it consist in a biaxial compression test that does not allow lateral deformation of the specimen, then the shear band formation is not possible. Nevertheless, several algorithms of fishtank has been used to develop the biaxial simulation with lateral soft boundary.

Fishtank biaxial environment

The fiishtank biaxial test consists in a set of procedures to: particle generation, set particle properties, seats the specimen (applying initial stresses), execute the load of the biaxial test with walls, and finally to get responses from the assembly.

The particle generation is made into a box of four walls with a radius expansion algorithm that allows defining the initial porosity of the specimen. First, with uniform distribution of particle radii and minimum and maximum radii defined, the algorithm computes the number of particles required inside the box based on the mean particle radius and the desired porosity, then the particles are generated and place randomly in the given sample area. The actual sample porosity is then calculated and the radii of all particles are increased by the following multiplication factor:

$$m = \sqrt{\frac{1 - n_{desired}}{1 - n_{measured}}} \tag{14}$$

where $n_{desired}$ and $n_{measured}$ are respectively, the desired and measured porosity. Expanding the radii by this factor will result in overlapping particles and, thus, large unbalanced forces. The particles are allowed to equilibrate on their own (without applied stresses). The particle assembly is created using zero friction and zero shear stiffness between particles. In this manner, no shear forces are generated between the particles in this initial state. After equilibrium is reached, particles are assigned friction values and shear stiffnesses. The sample is then allowed to re-equilibrate. Figure 1 show the particle generation process.

In the load process, the top and bottom walls act as loading platens, and the velocities walls are controlled by a servo-mechanism that maintains the reques-

Figure 1. Particle generation process. (a) Particle assembly after generating particles at half their final size (b) Particle assembly after equilibrium has reached (Itasca, 2002).

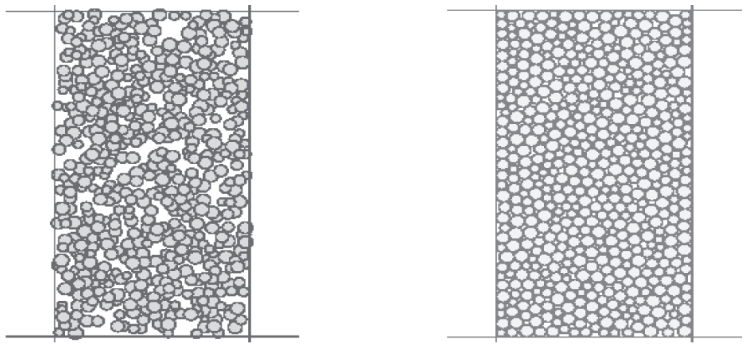

ted stresses. Accordingly with fish manual (Itasca, 2002), the biaxial test begins by applying confining and vertical stresses, next the dimensions of the specimen at this stage are taken as reference dimensions to be used in the computation of stresses and strains during subsequent load phase, the specimen is loaded by moving the platens towards one another at the velocity v_p. During load phase, the deviatoric stress, $\sigma_d = \sigma_y - \sigma_x$, and axial strain are monitored. The test ends when axial strain reach the specified limit ($\in_y < (\in_y)_{lim}$). Figure 2 shows a sketch of load process at the biaxial test.

Figure 2. Sketch of biaxial-test environment (Itasca, 2002).

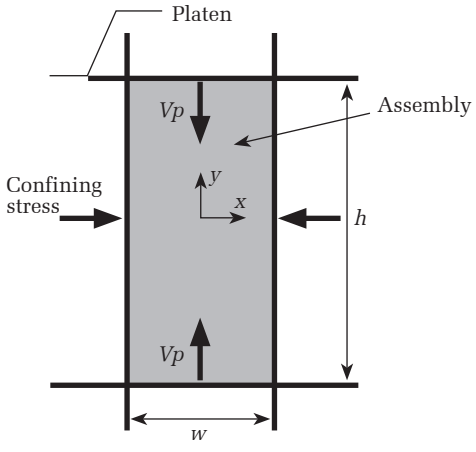

Control parameters

The input parameters that control the fish biaxial test are referred to define the material assembly and to control the boundary conditions and the end of the test. These parameters are listed in table 1.

Table 1. Parameters that control the fish biaxial simulation

Parameter	Description	Unit
ρ	Ball density	Kg/cm^3
η	Gross areal porosity	
Ec	Ball-ball contact modulus	Pa
k_n/k_s	Ball stiffness ratio	
μ	Ball friction coefficient	
H	Specimen height	m
W	Specimen width	m
β_x	Lateral wall stiffness-reduction factor	
β_y	Vertical wall stiffness-reduction factor	
σ_x^t	Target confining stress	Pa
σ_y^t	Target vertical stress	Pa
$\in$	Wall-servo tolerance	
v_p	Final platen velocity	m/s
N_p	Total cycles of platen acceleration	
S_p	Accelerate platens in this many stages	
$(\in_y)_{lim}$	Limiting vertical strain	

In table 1, the wall stiffness-reduction factors —are employed to set the wall normal stiffness as the factor for the average particle normal stiffness of the specimen. The wall-servo tolerance is used to control the wall velocity, such that corresponding velocity will be zero when $|(\sigma - \sigma^t)/\sigma^t| \leq \in$. Finally, the N_p and S_p parameters are used because if the platen velocity v_p is applied in a single step, the large acceleration will produce inertial forces within the specimen that may cause damage. To eliminate these inertial effects, the platen acceleration is controlled with the values of S_p and N_p. The platen velocity is adjusted to reach final value of v_p in a sequence of S_p stages over total of N_p cycles.

SOFT BOUNDARY ALGORITHM

Two kinds of particle control were implemented in algorithms to obtain soft boundary control with particles: velocity-controlled and force-controlled.

Velocity-controlled boundary

In a first approximation, after initial stress application with walls, behind of each wall a column was constructed with mono-sized particles. Particles in these columns were controlled with velocities of a similar procedure of wall servo-control. There were several difficulties: first, the indentation of boundary mono-sized particles caused a not realistic interaction between soft boundary and specimen (indentation of boundary particles into the specimen); second, it is not possible to monitor the confinement pressure for the indentation of particles and third, when one to fix velocity to boundary particle, also apply a force of undetermined magnitude; finally, the boundary particles increase the complexity of model and the calculation time. Although, shear band was not developed, the displacement field suggests localization (figure 3).

Table 2. Parameters of biaxial simulation with velocity-controlled soft boundary and complementary information

Parameter	Description	Value
ρ	Ball density	2630 Kg/cm^3
n	Gross areal porosity	0.14
Ec	Ball-ball contact modulus	88 x 10^9 Pa
k_n/k_s	Ball stiffness ratio	1.0
μ	Ball friction coefficient	0.5
R_{min}	Min. radius of ball assembly	7.5 x 10^{-4} m
R_{max}/R_{min}	Ratio max/min radius	1.66
H	Specimen height	64.01 x 10^{-3} m
w	Specimen width	32 x 10^{-3} m
β_x	Lateral wall stiffness-reduction factor	0.01
β_y	Vertical wall stiffness-reduction factor	1.0
σ_x^t	Target confining stress	10^6 Pa
σ_y^t	Target vertical stress	10^6 Pa
$\in$	Wall-servo tolerance	0.01
v_p	Final platen velocity	5.0 x 10^{-2} m/s
N_p	Total cycles of platen acceleration	400
S_p	Accelerate platens in this many stages	10
$(\in_y)_{lim}$	Limiting vertical strain	-1.5 x 10^{-2}
	Complementary information	
	Number of assembly balls	563
	Number of boundary balls	260
	Radius of boundary balls	2.5 x 10^{-4} m
	RAM memory	128 Mb
	Processor velocity	500 MHz
	Time of process	2.5 days

The parameters used in this simulation and other important information are listed in table 2.

Figure 3. Biaxial simulation with soft boundary velocity-controlled. (a) Final displacement field (b) Chain forces in assembly and boundary particle indentation.

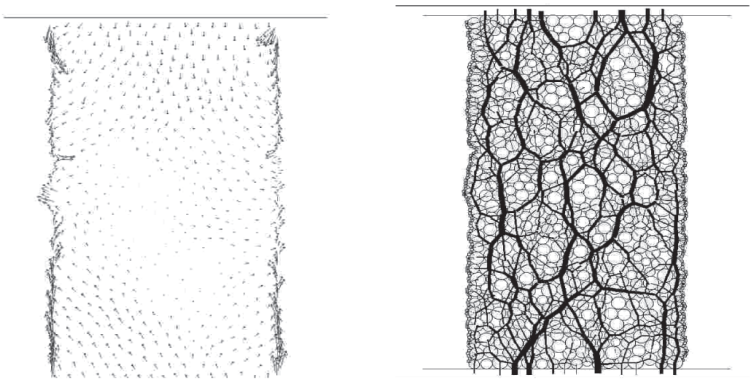

(a) (b)

Stress-controlled boundary

The second approximation of soft boundary consists in to identify and listing the boundary particles of the specimen, to get his contact forces with the lateral walls and boundary particle unbalanced force (horizontal component). To this purpose, it is necessary to generate several arrays to contain and to handle this information, and several control and monitoring procedures that lets to maintain the confinement pressure and to prevent damage or macro unbalanced condition of the specimen.

The procedure includes three steps: to initialize the membranes (boundary particles), to homogenize boundary forces to obtain a uniform stress condition and to control membrane; to monitor variables and prevents the lost of confinement pressure of the specimen in load phase.

Initializing the membrane

This procedure is applied after the initial stress application with walls. This one consists in to get the ball identification of the balls in contact with lateral walls by the list of contacts of the each lateral wall, next, to obtain the corresponding contact forces and particle's unbalanced forces. At this stage It was observe that the lateral forces on the boundary of the specimen are unbalanced (in very small magnitude but sufficient to cause lateral displacement of the specimen). Then, before to apply the forces on the balls that replace the confinement of the lateral walls, it is necessary to equilibrate the magnitudes of the confining forces on the boundary balls to the total force on the both membranes are equal.

Homogenization of boundary forces

In the final of last process, the magnitude of the applied forces on the boundary particles in the same membrane is very different particle to particle. To control the relative vertical displacement of the boundary particles and as the same time to maintain constant the confinement pressure it is necessary to modify magnitudes of boundary forces to obtain a uniform distribution of forces (uniform stress) over the membrane, but avoided inertial effect that damage the specimen.

On the other hand, to maintain the general equilibrium condition in specimen, the difference of the

sum of forces over membranes must remain null to allow the system equilibrium.

The procedure consists in: to get the relative height of each particle over each membrane. This height is the ratio between the external height of a boundary particle and the specimen height ($h_k^r = h_k^e/h$) as show in figure 4 where the k-particle belong to left membrane, then to compute the average and standard deviation of relative heights to each membrane; next in each calculation cycle, to compute the average and standard deviation of percentage of applied forces on the boundary particles, the corresponding normalized variable and comparing this one with average of normalized variable. If the normalized variable is larger than the average then the percentage of force of respective particle is reduced in a proportion of standard deviation of force percentages, else, a proportion of the sum of reductions of force percentages is added to the actual force percentage of the boundary particle. The homogenization process ends when the standard deviation of force percentage is smaller than the standard deviation of relative height in both membranes (Gómez, 2004).

To prevent the lost of local confinement of the specimen, the boundary particle x-velocity is fixed in zero.

With this process of homogenization, the chain forces before and after this process are equal.

Figure 4. Definition of particle external height in a left boundary particle.

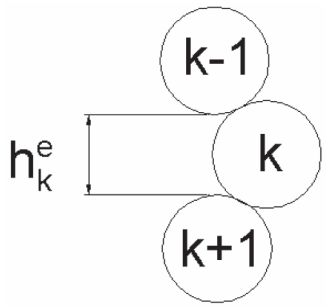

Control and monitoring

To control the confinement force during the axial load phase in biaxial test, if the assumption of uniform distribution of confinement pressure is true, the percentage of force applied to each boundary particle must be proportional to his relative height. Then, in each calculation cycle, it is necessary to compute the relative heights. But it is possible that inertial effects cause lost of contacts in some boundary (figure 5). To correct these inertial effect, in each calculation cycle, is assign zero velocity to the boundary particles but in the cycle the particle can to change his velocity for his unbalanced force.

In a simulation with the same control parameters of table 2, the final configuration and displacement field was the showed in figure 5.

With the model used was not possible to reproduce shear band but it is feasible loading laterally the specimen with the boundary particles after the particle generation and change the stiffness and friction of the particles, but it is necessary to check the internal sample equilibrium, for the inertial effect. It noted that always the minimum unbalanced force is around 10^{-6} or 10^{-7} Pa, then with the PFC2D simulations the internal perfect equilibrium never occurs.

Local fields of stress

To compute the evolution of local fields of stress, it is possible to implement local areas to obtain average stress tensors inside them. In each control area, are obtained the average of unbalanced forces of particles inside them, and this calculus can be develop several times during the axial loading process. If the control areas are defined small enough and are disposed over all specimen area, it is possible to obtain the local evolution of stress inside the specimen and "to fish" the shear band and his stress evolution.

Figure 5. Biaxial simulation with soft boundary stress-controlled. (a) Final displacement field (b) Chain forces and final assembly configuration (Gómez, 2004).

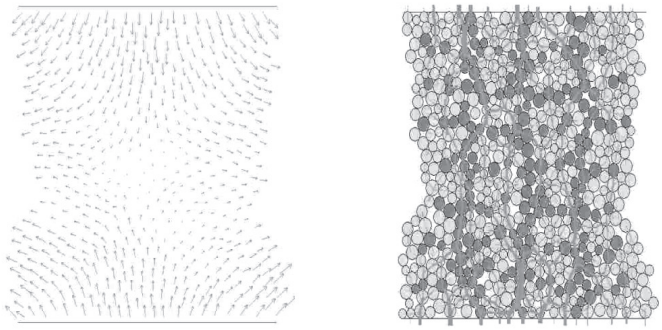

(a) (b)

Conclusions

Two soft boundary algorithms were implemented. The velocity-control boundaries do not allow the calculation of relevant macroscopic variables because the velocities on the boundary particles cause undetermined forces. The stress-controlled boundaries, allow the calculation of macroscopic variables but the correct control of confinement pressure was elusive. The inertial effects on PFC2D are difficult to control. It is possible to reproduce a shear band loading laterally the specimen with the boundary particles after the particle generation and change the stiffness and friction of the particles, but it is necessary to check the internal sample equilibrium, for the inertial effect caused by the walls during radius expansion process.

Bibliography

Bardet, J. P. & Proubet, J., A numerical investigation of the structure of persistent shear bands in granular media, *Géotechnique 41* (1991) No. 4, 599-613.

Bardet, J. P. & Proubet, J., The structure of shear bands in idealized granular materials, *Appl Mech Rev*, vol. 45, No. 3, part 2, March 1992, pp. S118-S122.

Bardet, J. P. & Proubet, J., Numerical simulations of shear bands in idealized granular materials, *Solid State Phenomena*, vol. 23 & 24, 1992, pp. 473-482.

Cundall, P. A., Strack, O. D. L., A discrete numerical model for granular assemblies, *Géotechnique 29* (1979), No. 1, 47-65.

Desrues, J., (1987), Naissance des bandes de cisaillement dans les milieux granulaires: expérience et théorie, *Manuel de rhéologie des géomatériaux* (Ed. Félix Darve). Presses de l'ecole nationale des Ponts et chaussées, pp. 279-298.

Gómez, A. Bandas de corte en materiales granulares: una aproximación micromecánica. Tesis de Maestría. Universidad de los Andes, 2004, 143 pág.

Han, C. & Vardoulakis, I. G., Plane-strain compression experiments on water-saturated fine-grained sand, *Géotechnique 41* (1991), No. 1, 49-78.

Hill, R., Acceleration waves in solids, *J. Mech. Phys. Solids 10* (1962), pp. 1-16.

Huang, W., Bauer, E. (2001), Numerical investigations of shear localization in a micro-polar hypoplastic material, *submitted to Int. J. Num. Anal. Meth. Geomech*.

Huang W., Nübel K. and Bauer E., Polar extension of a hypoplastic model for granular materials with shear localization, *Mechanics of Materials*, Sep 2002, vol. 34 Issue 9, p. 563, 14 p.

ITASCA Consulting Group, Inc., Particle Flow Code in 2 Dimensions – *Fish in PFC*. Software Manual PFC2D Version 3.0.

ITASCA Consulting Group, Inc., Particle Flow Code in 2 Dimensions – *Theory and Background*. Software Manual PFC2D Version 3.0.

Iwashita, K. & Oda, M., Rolling resistance at contacts in simulation of Shear Band development by DEM, *Journal of Engineering Mechanics*, March 1998, pp. 285-292.

Mandel, J. (1964). Propagation des surfaces de discontinuite dans un milieu elasto-plastique, Stress waves in anelastic solids. Springer-Verlag, Berlin.

Mühlhaus, H., Vardoulakis, I., The thickness of shear bands in granular materials, *Géotechnique 37* (1987), 271-283.

Oda, M. and Kazama H., Microstructure of shear bands and its relation to the mechanism of dilatancy and failure of dense granular soils, *Géotechnique 48* (1998), No. 4, 465-481.

Oda, M. & Iwashita, K., Study on couple stress and shear band development in granular media based on numerical simulation analyses, *International Journal of Engineering Science 38* (2000). 1713-1740.

Rudnicki, J. W., Rice, J. R., Conditions for the localization of deformation in pressure sensitive dilatants material, *J. Mech. Phys. Solids 23* (1975), pp. 371-394.

Tejchman, J, Gudehus, G.: Shearing of a narrow granular strip with polar quantities, *J. Num. and Anal. Meth. Geomech*. 25(2001), pp. 1-28.

Vardoulakis, I. & Sulem, J. (1995). *Bifurcation Análisis in Geomechanics*. Blackie Academic & Professional.